ELSEVIER

Desalination 145 (2002) 87–95

DESALINATION

www.elsevier.com/locate/desal

Derivation of adsorption parameters for nanofiltration membranes using a 1-pK Basic Stern model

W.B. Samuel de Lint[a], Nieck E. Benes[a]*, Arnoud P. Higler[b], Henk Verweij[c]

[a]*Inorganic Materials Science Group, Department of Chemical Technology & Mesa+ Research Institute, University of Twente, P.O. Box 217, 7500 AE Enschede, The Netherlands*
Tel. +31 53 489 5419; Fax +31 53 489 4683; email: w.b.s.delint@ct.utwente.nl, n.e.benes@ct.utwente.nl.
[b]*Shell Global Solutions International B.V., Badhuisweg 3, 1031 CM Amsterdam, The Netherlands*
email: arnoud.higler@shell.com.
[c]*Department of Materials Science and Engineering, The Ohio State University, 2041 College Road, 291 Watts Hall, Columbus, OH 43210-1178, USA, email: verweij@mse.eng.ohio-state.edu.*

Received 5 February 2002; accepted 4 March 2002

Abstract

The ion retention and flux of nanofiltration (NF) membranes are to a large extent determined by the membrane surface charge. This surface charge is in turn strongly influenced by adsorption of ions from the solution onto the membrane material. A 1-pK adsorption model with a Basic Stern electrostatic double layer model is used to describe ion adsorption, and the sensitivity of this model for various parameters is discussed. From a non-linear regression analysis of literature data [1,2] regarding the surface charge and the zeta-potential, adsorption parameters for the 1 pK model are obtained for sodium chloride on γ-alumina.The 1-pK Basic Stern model could predict the surface charge well, except for the highest concentration of 1000 mol/m^3. Reasonable agreement is found between the measured zeta-potentials and the model predictions.

Keywords: Specific adsorption; Nanofiltration membranes; Zeta-potential; Surface charge; γ-alumina

1. Introduction

Nanonfiltration (NF) of electrolyte solutions is mainly determined by electrostatic effects, which are governed by the surface charge of the membrane. The surface charge depends on the composition of the solution (concentrations, pH) and adsorption parameters. These parameters can be determined from a variety of methods, including potentiometric

*Corresponding author.

Presented at the International Congress on Membranes and Membrane Processes (ICOM), Toulouse, France, July 7–12, 2002.

PII: S0011-9164(02)00391-0

titration and electrophoretic mobility [1,3], acoustic techniques [4], or by the use of colloidal probe or surface-force techniques [5], and can be used in transport models for predicting membrane separation behaviour [6–10], that is, ion retention and flux.

Numerous adsorption models for oxides have been presented in literature such as the porous gel model [11] and several site-binding models [e.g. 12–14]. We will restrict the discussion to a site-binding model in which the charged surface is thought to consist of discrete surface sites that can interact with the various ions in the electrolyte solution. Generally it is assumed that the surface is in thermodynamic equilibrium with the solution phase next to the surface, as well as with the bulk solution. Furthermore, we consider a simple 1-pK adsorption scheme, in which the hydroxyl surface groups are charged [15–17] and can only adsorb a proton (i.e., desorption of protons from hydroxyl surface sites is not considered), and an electrostatic Basic Stern model [15,18]. Other site binding models may be equally appropriate (see [19]). Subsequent to a parametric study, the 1-pK Basic Stern model is combined with a non-linear regression algorithm and applied to literature data [1, 2] for the surface charge and the zeta potential of γ-alumina in a NaCl solution at various pH to extract the corresponding adsorption parameters.

2. Theory

Inorganic NF membranes generally consist of oxides (e.g., Al_2O_3, TiO_2, ZrO_2), which form surface hydroxyl groups [–OH] in aqueous solutions. These groups are considered to be the adsorption sites at which competitive adsorption of ions (including H^+) can occur. In this work the discussion is restricted to a simple adsorption scheme in which the hydroxyl surface groups are charged [15–17] and can only adsorb a proton (i.e., no desorption of protons from hydroxyl surface sites occurs). Cations (C^+) and anions (A^-) then adsorb on the formed charged sites (extension to multivalent ions is straightforward). This model is often referred to as the 1-pK model [15]. The corresponding surface reactions are

$$\begin{aligned} &\mathrm{Al\text{-}OH_2^{+1/2}} + \mathrm{H^+}(s) \xleftrightarrow{K^+} \mathrm{Al\text{-}OH_2^{+1/2}} \\ &\mathrm{Al\text{-}OH^{-1/2}} + \mathrm{C^+}(s) \xleftrightarrow{K_C} \mathrm{Al\text{-}OH^{-1/2}C^+} \\ &\mathrm{Al\text{-}OH_2^{+1/2}} + \mathrm{A^-}(s) \xleftrightarrow{K_A} \mathrm{Al\text{-}OH^{+1/2}A^-} \end{aligned} \quad (1)$$

where (s) refers to ions that are not adsorbed but reside very near the surface plane of the material. γ-alumina will be used as a reference material in this paper. The equilibrium constants K for these reactions are

$$K^+ = \frac{c_{\mathrm{Al\text{-}OH_2^{+1/2}}}\, c^{\mathrm{ref}}}{c^s_{\mathrm{H^+}}\, c_{\mathrm{Al\text{-}OH^{-1/2}}}}, K_C = \frac{c_{\mathrm{Al\text{-}OH^{-1/2}C^+}}\, c^{\mathrm{ref}}}{c^s_{\mathrm{C^+}}\, c_{\mathrm{Al\text{-}OH^{-1/2}}}},$$
$$K_A = \frac{c_{\mathrm{Al\text{-}OH_2^{+1/2}A^-}}\, c^{\mathrm{ref}}}{c^s_{\mathrm{A^-}}\, c_{\mathrm{Al\text{-}OH_2^{+1/2}}}} \quad (2)$$

where c_i^s are the concentrations of the surface complexes [mol/m^2], and c^{ref} is the thermodynamic reference concentration of 10^3 mol/m^3 (1 mol/dm^3).

The electrostatic double layer model adopted in this study is a two-layer model; an empty Helmholtz layer directly at the surface and a diffuse (Gouy-Chapman) double layer, which is displaced from the Helmholtz layer by a certain distance (see Fig. 1). The model is generally referred to as the Basic Stern (BS) model, and has been widely accepted as applicable for AgI systems [15, 19]. In the BS model, protons (or hydroxyl ions) adsorb directly at the surface, screening some of the surface charge σ_0. Due to their size, cations and anions adsorb at a plane located at the tail end of the Helmholtz layer (1-plane).

The surface concentrations are related to the bulk concentrations using the Boltzmann equation

$$c^s_{\mathrm{H^+}} = c^b_{\mathrm{H^+}} \exp\left(\frac{-F}{RT}\psi_0\right), c^s_{\mathrm{C^+}} = c^b_{\mathrm{C^+}} \exp\left(\frac{-F}{RT}\psi_1\right),$$
$$c^s_{\mathrm{A^-}} = c^b_{\mathrm{A^-}} \exp\left(\frac{-F}{RT}\psi_1\right) \quad (3)$$

where c_i^b is the bulk concentration of species i

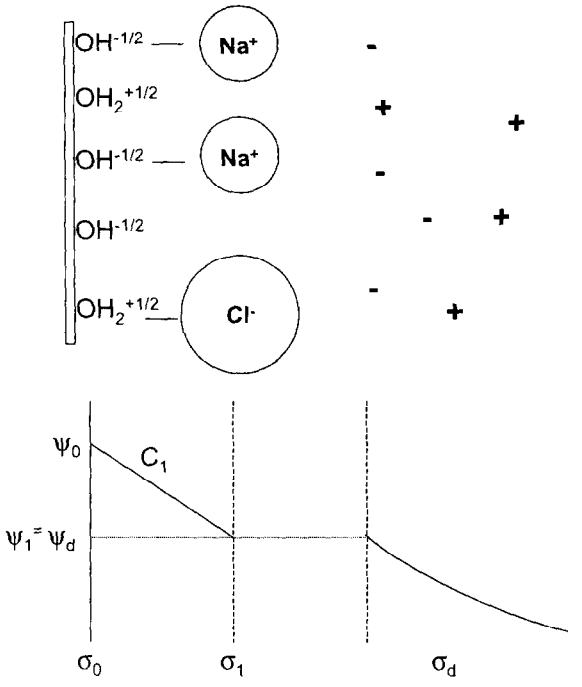

Fig. 1. Schematic representation of the electrostatic double layer model.

[mol/m^3] and the choice for either ψ_0 or ψ_1 is determined by the plane a species is located in.

For the BS model, the surface charge σ_0 is

$$\sigma_0 = \frac{F}{2}\left(c_{\text{Al-OH}_2^{+1/2}} - c_{\text{Al-OH}^{-1/2}} + c_{\text{Al-OH}_2^{+1/2}\text{A}^-} - c_{\text{Al-OH}^{-1/2}\text{C}^+}\right) \quad (4)$$

Note that we have two types of sites in the 0-plane, free sites (Al-OH$^{-1/2}$, Al-OH$_2^{+1/2}$) and occupied sites (Al-OH$^{-1/2}$C$^+$, Al-OH$_2^{+1/2}$A$^-$), which both sites contribute to σ_0. The surface charge is partly compensated by specific adsorption of cations and anions in the tail end of the Helmholtz layer,

$$\sigma_0 = C_1(\psi_0 - \psi_1) \quad (5)$$

where C_1 is the differential or Helmholtz capacity.

The remaining surface charge has to be compensated in the diffuse double layer [15,19]

$$\sigma_1 = F\left(c_{\text{Al-OH}^{-1/2}\text{C}^+} - c_{\text{Al-OH}_2^{+1/2}\text{A}^-}\right) \quad (6)$$

$$\sigma_1 = -(\sigma_0 + \sigma_d) = C_1(\psi_1 - \psi_0) + \text{sign}(\psi_1)\sqrt{2\varepsilon_0\varepsilon_r RT\sum_{i=1}^{n} c_i^b\left[\exp\left(\frac{-z_i F}{RT}\psi_1\right) - 1\right]} \quad (7)$$

with σ_d the charge in the diffuse double layer, sign (ψ_1) the sign of ψ_1 (+1 or −1), ε_0 the permittivity of vacuum, ε_r the relative permittivity (ε_r = 78 for water), R the ideal gas constant, T the temperature, z_i the charge number of species i, and F the Faraday constant. The summation in Eq. (7) has to be performed over all mobile (i.e. bulk) species, n, this means including the bulk protons and hydroxyl ions.

The bulk concentrations of protons (formally H_3O^+) and hydroxyl ions are not independent but related by the water autoprotolysis equilibrium reaction

$$H_2O \xleftrightarrow{K_w} H^+ + OH^- \qquad K_w = c^b_{H^+}c^b_{OH^-} \quad (8)$$

In writing Eq. (7) we have assumed that the bulk solution is in thermodynamic equilibrium with any position in the electrostatic double layer, the bulk solution is thermodynamically ideal, the double layer thickness is much smaller than the radius of the particle, a relative permittivity independent of the electric field (ε_r = 78 [20]) and isolated surfaces. Also, we set the electrostatic potential in the bulk equal to zero.

The adsorption model is completed by an expression for the total fixed number of surface sites c^s_{tot},

$$c^s_{\text{tot}} = \left(c_{\text{Al-OH}^{-1/2}} + c_{\text{Al-OH}_2^{+1/2}} + c_{\text{Al-OH}^{-1/2}\text{C}^+} + c_{\text{Al-OH}_2^{+1/2}\text{A}^-}\right) \quad (9)$$

Eqs. (2–9) is a set of 8 relations containing 8 variables ($c_{\text{Al-OH}^{-1/2}}$, $c_{\text{Al-OH2}^{+1/2}}$, $c_{\text{Al-OH}^{-1/2}\text{C}^+}$, $c_{\text{Al-OH2}^{+1/2}\text{A}^-}$,

σ_0, σ_1, ψ_0 and ψ_1) that can be solved for a given set of adsorption parameters (K^+, K_C, K_A, C_1, c^s_{tot}) and bulk concentrations c^b_i [19]. By utilising a minimisation algorithm the adsorption parameters can be changed to achieve optimal agreement between model and experiment. Variables that are experimentally available are σ_0 (from titration experiments, [1,3]), σ_1 (from radiotracer techniques, [2]), ψ_0 (potential characteristics on ISFETS, [21]) or ψ_1 (from zeta-potential measurements on isolated particles, [1,3,4], if $\psi_1 = \zeta$). In this work we will use the Simplex minimisation algorithm (Nelder and Mead [22]) to connect the adsorption parameters to experimental data.

3. Results and discussion

The sensitivity of the charge and potential predicted by the 1-pK Basic Stern model for the adsorption parameters is numerically investigated. Second, the minimisation algorithm is used to obtain values for the adsorption parameters from literature data. The sensitivity analysis is based on a 1–1 10.0 mol/m^3 electrolyte interacting with an oxidic material, at different pH values (Table 1).

Table 1
Data used in the simulations for the base case

$pK^+ = -8.0$, $pH^{pzc} = 8.0$ (γ-alumina, [1])
$pK_C = pK_A = 8.0$, $C_1 = 1.4$ C/(V·m^2)
$c^s_{tot} = 8.3 \cdot 10^{-6}$ mol/m^2 (i.e. 5.0 sites/nm^2, [27])
For the feed solution $c^f = 10.0$ mol/m^3,
$K_w = 1 \cdot 10^{-8}$·mol^2/m^6
$F = 96485$ C/mol, $R = 8.3144$ J/(mol·K), $T = 298.15$ K
$\varepsilon_0 = 8.854 \cdot 10^{-12}$ C/(V·m), $\varepsilon_r = 78$

3.1. Influence of proton affinity constant, K^+

An increase in K^+ yields a higher surface charge at each pH. At a certain pH the surface charge is zero ($\sigma_0 = 0$). This pH is referred to as the points of zero charge (pzc) [23]. Similarly, the pH at which $\sigma_0 + \sigma_1 = 0$ is called isoelectric point (iep). Fig. 2 shows that increasing K^+ shifts σ_0, ψ_0 and ψ_1 to higher pH (pzc and iep are both increased). According to Eq. (5), a rise in surface charge ($\sigma_0\uparrow$) requires $(\psi_0 - \psi_1)\uparrow$, as can be observed in Fig. 2a. Since we set $K_C = K_A \approx 0$ for the simulations presented in Fig. 2, $\sigma_0 = -\sigma_d$ ($\sigma_1 \approx 0$). Consequently, $\sigma_0\uparrow$ results in $\sigma_d\downarrow$. From Eq. (7) it is clear that the decrease of charge in the double layer ($\sigma_d\downarrow$) corresponds to an increase in the potential at plane 1 ($\psi_1\uparrow$). From $(\psi_0 - \psi_1)\uparrow$ and $\psi_1\uparrow$ it follows that the surface potential should increase ($\psi_0\uparrow$), and rise more strongly than the potential at plane 1 ($\Delta\psi_0 > \Delta\psi_1$, see Fig. 2b).

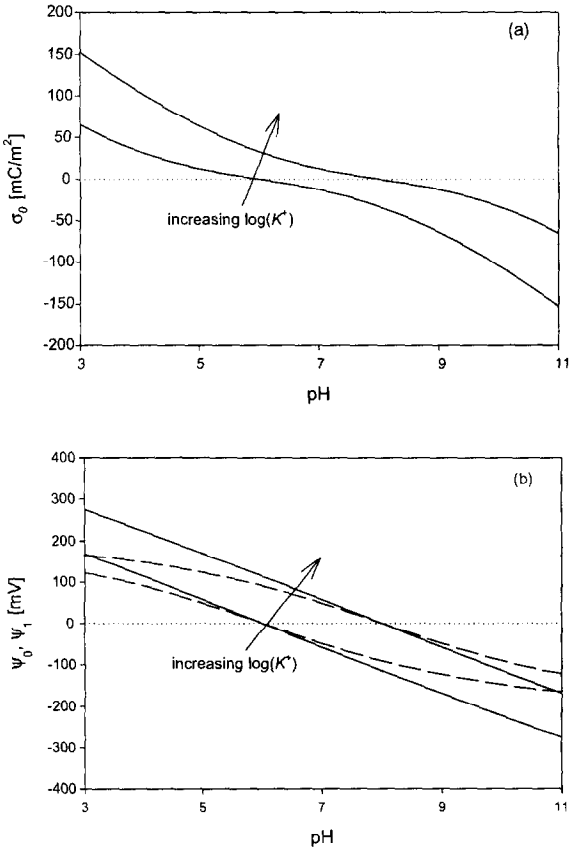

Fig. 2. Dependence of (a) the surface charge and (b) the surface potential (solid lines), the 1-plane potential (dashed lines) on log (K^+) for log (K^+) values of 6.0 and 8.0 (base case). Other parameters in Table 1.

3.2. Degree of cation adsorption, K_C

Fig. 3 shows that an increase of K_C is only visible in σ_0, σ_1 and ψ_1 and at high pH values (basic region). The surface charge decreases, while σ_1 and ψ_1 increase (ψ_0 increases as well, but only marginally). This is because in this region σ_0 and σ_1 are almost completely determined by the number of Al-$OH^{-1/2}$ and Al-$OH^{-1/2}C^+$ species (the protonated and anion-complex species concentrations are very small). At high pH and for increasing K_C [see Eq. (4)], σ_0 decreases and σ_1 increases (Fig. 3a), but the surface charge decreases less than the 1-plane charge,

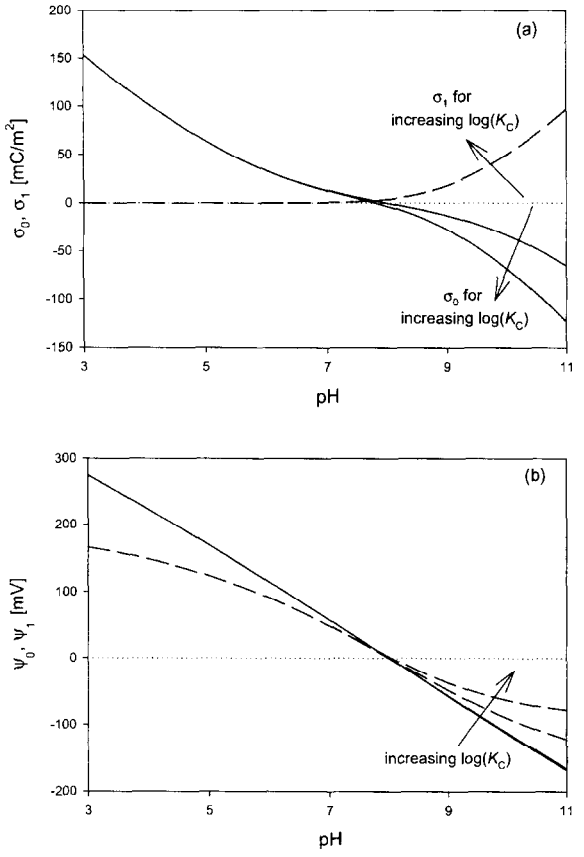

Fig. 3. Dependence of (a) the surface charge (solid lines), the 1-plane charge (dashed lines) and (b) the surface potential (solid lines), the 1-plane potential (dashed lines) on log (K_C) for log (K_C) values of 0.0 and –8.0 (base case). Other parameters in Table 1.

$\Delta\sigma_1 > \Delta\sigma_0$. Initially, K_C and K_A were set to be almost equal to zero (i.e. $\sigma_1 \approx 0$) and hence the concentration of Al-$OH^{-1/2}C^+$ and Al-$OH_2^{+1/2}A^-$ species was very low. With increasing K_C, however, cations compete with protons for the Al-$OH^{-1/2}$ adsorption sites. If $K_C\uparrow$, cations will replace the protons on the surface groups (Al-$OH_2^{+1/2}$ → Al-$OH^{-1/2}C^+$), resulting in a lower surface charge (i.e. $\sigma_0\downarrow$). Since at high pH there were already few Al-$OH_2^{+1/2}$ groups at the surface, this effect of proton replacement by cations is rather limited in the 0-plane. The surface charge in the 1-plane is, however, directly proportional to the number of Al-$OH^{-1/2}C^+$ groups and σ_1 will consequently rise more than σ_0 decreases ($\Delta\sigma_1 > \Delta\sigma_0$).

Because the decrease in surface charge is less than the rise in σ_1, the diffuse double layer charge decreases ($\sigma_d\downarrow$). Less charge in the diffuse double layer implies that the 1-plane potential, ψ_1, has to increase. Since σ_0 decreases, consequently ($\psi_0 - \psi_1$) has to go down. Because of the competition with cations, the concentration of protons in the 0-plane will go down and, according to Eq. (3), this implies that the surface potential has to increase at pH>pzc (were $\psi_0 < 0$), $\psi_0\uparrow$ (i.e. it becomes less favourable for the protons to be situated near the surface). The behaviour for ψ_0 and ψ_1 is shown in Fig. 3b, though the change in the surface potential is hardly visible.

The behaviour of σ_0, σ_1, ψ_0 and ψ_1 for increasing values of the anionic equilibrium constant (K_A) is the reverse (not shown) of that for increasing K_C. Here the effects of K_A are largest in the low pH range (acidic region).

3.3. Helmholtz capacity dependence, C_1

The Helmholtz capacity is defined by the ratio of vacuum and relative permittivity over the thickness of the Helmholtz layer d [18,23,24].

$$C_1 = \frac{\varepsilon_0 \varepsilon_r}{d} \tag{10}$$

When C_1 approaches large values it means that the thickness of the Helmholtz layer decreases. As a result, the 1-plane potential and surface potential should move closer together, that is, $(\psi_0 - \psi_1)\downarrow$. For pH>pzc, ψ_0 is negative and more negative than ψ_1, and consequently ψ_1 will decrease for increasing C_1. For pH values below the pzc the situation is reversed (initially $\psi_0>0$, $\psi_1>0$ and $\psi_0>\psi_1$) and ψ_1 should increase when the capacity increases. Both effects are clearly shown in Fig. 4b.

For the capacitance simulations, K_C and K_A were set to almost zero and it follows that the 1-plane charge is almost zero and the surface charge is completely compensated in the diffuse double layer (i.e. $\sigma_0 = -\sigma_d$). The diffuse double layer charge is directly related to the 1-plane potential [Eq. (7)] and follows the reverse behaviour described for ψ_1: for high pH ($\psi_1\downarrow$), σ_d increases and for low pH ($\psi_1\uparrow$), σ_d decreases. Because the surface charge behaves opposite to σ_d, σ_0 is expected to decrease for high pH and increase for low pH (see Fig. 4a).

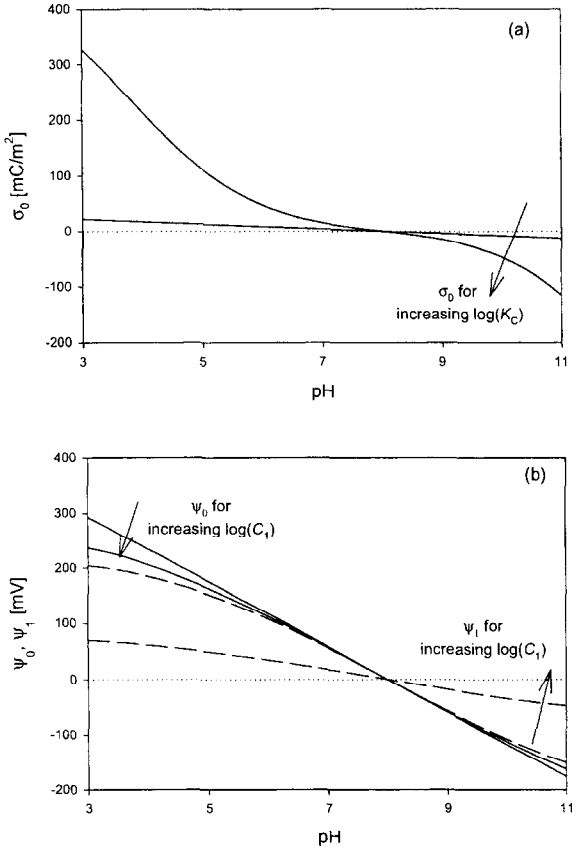

Fig. 4. Dependence of (a) the surface charge and (b) the surface potential (solid lines), the 1-plane potential (dashed lines) on the Helmholtz capacity (C_1) for C_1 values of 0.1 and 10.0 C/(V·m²). Other parameters in Table 1.

3.4. Deriving adsorption parameters from literature data

Sprycha [1] performed measurements of the surface charge and the zeta-potential (defined as the potential located at the shear plane of an interface) for monovalent electrolytes on γ-alumina as a function of pH. We applied our adsorption model to the data of Sprycha. For the fitting of σ_0 this was quite straightforward since this variable follows directly from the electrostatic model [see Eq. (5), ψ_0 and ψ_1 are determined by the model]. For ζ we assumed that it is situated at the head-end of the diffuse double layer (i.e. $\zeta = \psi_1$). In the fitting procedures for σ_0 and ζ we have kept the values of K^+ and c^s_{tot} fixed since K^+ follows directly from the pzc ($\sigma_0 = 0$) and c^s_{tot} is highly correlated to the other parameters, hence it cannot be determined from these experimental data. We have used $c^s_{tot} = 1.33\cdot10^{-5}$ mol/m² (i.e. 8 sites/nm²) as obtained from infrared experiments [25].

The adsorption model yields good predictions for the surface charge as function of pH (Fig. 5a). Only at high concentrations of 1000 mol/m³ the fit deteriorates. When the model parameters from Fig. 5a are used to calculate the zeta-potential (i.e ψ_1), ζ is underestimated (plot not shown), though predictions are much better than for the reversed procedure. The fit for the zeta-potential is rather poor (Fig. 5b). The model is not capable of describing the limiting ζ values at very high and low pH. Also, if we use the obtained parameters to calculate the surface charge, they grossly underestimate σ_0 (up to 5x as low) as found from titration experiments (comparison not shown). The model parameters that were calculated for

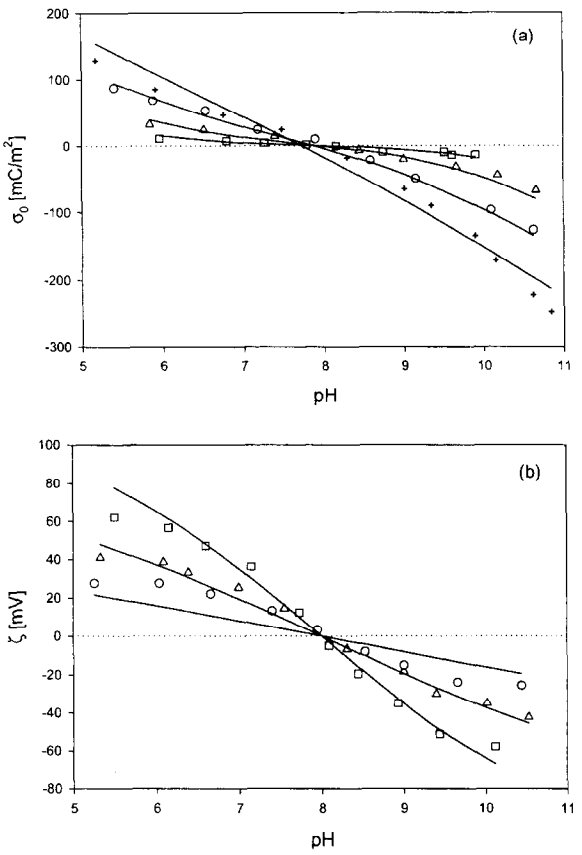

Fig. 5. 1-pK BS model fit (solid lines) based on data from Sprycha [1,2] for adsorption of NaCl on γ-alumina: 1 mol/m^3 (squares), 10 mol/m^3 (triangles), 100 mol/m^3 (circles) and 1000 mol/m^3 (crosses). (a) Surface charge (σ_0), log (K^+)=8.0, log (K_C)=–1.0, log (K_A)=–2.5, C_1=1.6C/(V·m^2), c^s_{tot} = 1.33·10^5 mol/m^2 (8.0 sites/nm^2) [25]. (b) Zeta-potential (ζ), ζ = ψ_1, log (K^+) = 8.0, log (K_C) = –8.7, log (K_A) = –2.2, C_1 = 0.12 C/(V·m^2), c^s_{tot} = 1.33·10^5 mol/m^2 (8.0 sites/nm^2) [25].

the fit of σ_0 (Fig. 5a) are, however, very different from the results found for the zeta-potential fit. Apart from the poor fit for ζ, it was possible to obtain multiple solutions that described the experimental data equally well. Instead of log (K_C) = –8.7 and log (K_A) = –2.2 (see Fig. 5b) the same model data set could be obtained with the parameters log (K_C) = –10.6 and log (K_A) = –2.5 (all other parameters remained constant). The absence of a unique parameter solution is known from model investigations in literature [19,26].

The observed model behaviour is not typical for this case, however. A consistent description of the surface charge and zeta-potential within the framework of one site-binding model has proven to be quite difficult [13,18]. Model predictions can sometimes be improved by using a more elaborate double layer model or multiple adsorption sites, but is questionable if this approach improves the physical representation of the oxide material, even more so when we would like to describe adsorption in inorganic NF membranes that consist of highly porous materials. For materials with a high porosity it is uncertain if the Helmholtz capacity [Eq. (5)] can still be considered constant [18]. Also, we argue that the assumptions used to arrive at the diffusive double layer charge [second term in Eq. (7)] require careful attention.

4. Conclusions

A 1-pK adsorption model was combined with a Basic Stern electrolyte double layer model and used to describe adsorption of ions on an oxidic surface to derive the adsorption parameters for application in a transport model for NF membranes. The dependence of the surface charge, σ_0, and the 1-plane potential, ψ_1, on the model parameters was investigated. Also the model was applied to extract adsorption parameters from an experimental study of sodium chloride adsorption on γ-alumina. When the model was fitted to the experimental ζ-potential data the model parameters were log (K^+) = 8.0, log (K_C) = –8.7, log (K_A) = –2.2, C_1 = 0.12 C/(V·m^2), c^s_{tot} = 1.33·10^{-5} mol/m^2 (i.e. 8.0 sites/nm^2). Estimated model parameters for the surface charge measurements were log (K^+) = 8.0, log (K_C) = –1.0, log (K_A) = –2.5, C_1 = 1.6 C/(V·m^2), c^s_{tot} = 1.33·10^{-5} mol/m^2 (8.0 sites/nm^2). Discrepancies between the parameter predictions and the surface charge or zeta-potential obtained with both methods are caused by the lack of knowledge about the physical properties of the oxide material as well as by questionable assumptions made in the site-binding model. Still, the model predicts

surface charge and zeta-potential qualitatively and may be suitable for the description of surface adsorption behaviour in nanofiltration membranes.

Symbols

C_1 — Helmholtz capacity, C/(V·m²)
c_i — Concentration of adsorbed surface species i, mol/m²
c^{ref} — Thermodynamic reference concentration, mol/m³
c^s_i — Surface concentration of non-adsorbed ions i,mol/m³
c^b_i — Bulk concentration of species i, mol/m³
c^s_{tot} — Total concentration of surface sites, mol/m²
F — Faraday constant, C/mol
K^+ — Proton adsorption equilibrium constant
K_A — Anion adsorption equilibrium constant
K_C — Cation adsorption equilibrium constant
K_w — Water autoprotolysis equilibrium constant, mol²/m⁶
R — Ideal gas constant, J/mol·K
T — Temperature, K
z_i — Charge number of species i

Greek

ε_0 — Vacuum permittivity, C/(V·m)
ε_r — Relative permittivity
σ_0 — Surface charge, C/m²
σ_1 — Charge at the 1-plane, C/m²
σ_d — Diffuse double layer charge, C/m²
ψ_0 — Surface potential, V
ψ_1 — Potential at the 1-plane,V
ζ — Zeta-potential, V

References

[1] R. Sprycha, Electrical double layer at alumina/electrolyte interface. I. Surface charge and zeta potential, J. Colloid Interface Sci., 127 (1989) 1–11.
[2] R. Sprycha, Electrical double layer at alumina/electrolyte interface. II. Adsorption of supporting electrolyte ions, J. Colloid Interface Sci., 127 (1989) 12–25.
[3] C.-P. Huang and W. Stumm, Specific adsorption of cations on hydrous γ-Al_2O_3, J. Colloid Interface Sci., 43 (1973) 409–420.
[4] S.B. Johnson, P.J. Scales and T.W. Healy, The binding of monovalent electrolyte ions on α-alumina. I. Electroacoustic studies at high electrolyte concentrations, Langmuir, 15 (1999) 2836–2843.
[5] B.V. Zhmud, A. Meurk and L. Bergström, Evaluation of surface ionization parameters from AFM data, J. Colloid Interface Sci., 207 (1998) 332–343.
[6] M.S. Hall, V.M. Starov and D.R. Lloyd, Reverse osmosis of multicomponent electrolyte solutions. Part I. Theoretical development, J. Membr. Sci., 128 (1997) 23–37.
[7] M.S. Hall, D.R. Lloyd and V.M. Starov, Reverse osmosis of multicomponent electrolyte solutions. Part II. Experimental verification, J. Membr. Sci., 128 (1997) 39–53.
[8] V.M. Starov, W.R. Bowen and J.S. Welfoot, Flow of multicomponent electrolyte solutions through narrow pores of nanofiltration membranes, J. Colloid Interface Sci., 240 (2001) 509–524.
[9] P.M. Biesheuvel and W.B.S. De Lint, Application of the charge regulation model to the separation of ions by hydrophilic membranes, J. Colloid Interface Sci., 241 (2001) 422–427.
[10] W.B.S. De Lint, P.M. Biesheuvel and H. Verweij, Application of the charge regulation model to transport of ions through hydrophilic membranes. One-dimensional transport model for narrow pores (nanofiltration), submitted to J. Colloid Interface Sci. (2002).
[11] J. Lyklema, The electrical double layer on oxides, Croat. Chem. Acta., 43 (1971) 249–260.
[12] T.W. Healy and L.R. White, Ionizable surface group models of aqueous interfaces, Adv. Colloid Interface Sci., 9 (1978) 303–345.
[13] J.A. Davis, R.O. James and J.O. Leckie, Surface ionization and complexation at the oxide/water interface. I. Computation of electrical double layer properties in simple electrolytes, J. Colloid Interface Sci., 63 (1978) 480–499.
[14] D.E. Yates, S. Levine and T.W. Healy, Site-binding model of the electrical double layer at the oxide/water interface, J. Chem. Soc. Faraday Trans. I, 70 (1974) 1807–1818.
[15] T. Hiemstra, W.H. van Riemsdijk and M.G.M. Bruggenwert, Proton adsorption mechanism at the gibbsite and aluminium oxide solid/solution interface, Neth. J. Agric. Sci., 35 (1987) 281–293.

[16] T. Hiemstra, W.H. van Riemsdijk and G.H. Bolt, Multisite proton adsorption modeling at the solid/solution interface of (hydr)oxides: a new approach. I. Model description and evaluation of intrinsic reaction constants, J. Colloid Interface Sci., 133 (1989) 91–104.

[17] T. Hiemstra, J.C.M. de Wit and W.H. van Riemsdijk, Multisite proton adsorption modeling at the solid/solution interface of (hydr)oxides: a new approach. II. Application to various important (hydr)oxides, J. Colloid Interface Sci., 133 (1989) 105–117.

[18] T. Hiemstra, H. Yong and W.H. van Riemsdijk, Interfacial charging phenomena of aluminium (hydr)oxides, Langmuir, 15 (1999) 5942–5955.

[19] J. Westall and H. Hohl, A comparison of electrostatic models for the oxide/solution interface, Adv. Colloid Interface Sci., 12 (1980) 265–294.

[20] S. Basu and M.M. Sharma, An improved space-charge model for flow through charged microporous membranes, J. Membr. Sci., 124 (1997) 77–91.

[21] L. Bousse, N.F. de Rooij and P. Bergveld, The influence of counter-ion adsorption on the ψ_0/pH characteristics of insulator surfaces, Surf. Sci., 135 (1983) 479–496.

[22] W.H. Press, S.A. Teukolsky, W.T. Vetterling and B.P. Flannery, Numerical Recipes in Fortran 77, 2nd ed., Cambridge University Press, Cambridge, 1992, pp. 402–406.

[23] J. Lyklema, Fundamentals of Interface and Colloid Science. Vol.2: Solid-Liquid Interfaces, Academic Press, London, 1995, pp. 3.107–3.109.

[24] J.O.M. Bockris, A.K.N. Reddy and M.Gamboa-Aldeco, Modern Electrochemistry 2A. Fundamentals of Electrodics, 2nd ed., Kluwer Academic/Plenum Publishers, New York, 2000, pp. 871–887.

[25] N. Sahai and D.A. Sverjensky, Evaluation of internally consistent parameters for the triple-layer model by the systematic analysis of oxide surface titration data, Goechim. Cosmochim. Acta, 61 (1997) 2801–2826.

[26] L.K. Koopal, W.H. van Riemsdijk and M.G. Roffey, Surface ionization and complexation models: a comparison of methods for determining model parameters, J. Colloid Interface Sci., 118 (1987) 117–136.

[27] D.Y.C. Chan, J.W. Perram, L.R. White and T.W. Healy, Regulation of surface potential at amphoteric surfaces during particle-particle interaction, J. Chem. Soc. Faraday Trans. I, 71 (1975) 1046–1057.